Laser Temperature-Jump Study of Stacking in Adenylic Acid Polymers†

T. G. Dewey and Douglas H. Turner*

ABSTRACT: The kinetics of the single-strand stacking of adenylic acid polymers have been investigated by using the laser temperature-jump method. This technique allowed the determination of rate constants for polyriboadenylic acid [poly(A)], the riboadenylic acid heptamer, and polydeoxyriboadenylic acid [poly(dA)] at 0.05 M ionic strength. At this low ionic strength a single, wavelength-independent relaxation is observed for the ribopolymers. The thermodynamics were determined from an analysis of the melting curves measured by ultraviolet absorption. By assumption of a two-state model, the rate constants for formation of the stacked state at 25 °C for poly(A) and poly(dA) are 0.7×10^7 and 2.7×10^7 s^{-1}, respectively. The reverse rate constants are 3.2×10^6 s^{-1} for poly(A) and 4.3×10^6 s^{-1} for poly(dA). The activation energy for poly(A) was 4.0 kcal/mol for the forward rate and 15.2 kcal/mol for the reverse rate. Poly(dA) has a similar activation energy of 3.2 kcal/mol for the forward rate and a lower reverse rate activation energy of 12.3 kcal/mol. The ribo heptamer results are similar to poly(A). The forward rate constants are relatively small considering the low activation barriers. This is interpreted as a conformational effect on the activation entropy. At 0.2 M ionic strength with 0, 2, or 5 mM Mg^{2+}, poly(A) exhibits a wavelength dependence to the relaxation time. This indicates the presence of more than two states. At these high salt concentrations, the relaxation times are longer than at 0.05 M ionic strength. This is interpreted as a decrease in the rate of unstacking. Thus, high salt appears to stabilize the stacked state.

The conformational dynamics of nucleic acids have been investigated by a variety of techniques. In general, the time scale of these processes increases with their complexity. Proton and phosphorus NMR have shown backbone rotations to be in the 10^{-8}–10^{-10}-s regime (Akasaka, 1974; Davanloo et al., 1979). Ultrasonic measurements on syn–anti isomerization in adenosine reveal relaxation times on the order of 10^{-9} s (Rhodes & Schimmel, 1971; Hemmes et al., 1974). The stacking of bases in polyadenylic acid [poly(A)][1] takes 10^{-6}–10^{-7} s (Pörschke, 1973, 1978), and double-stranded helix formation in oligomers ranges from about 10^{-3} to 10^{-1} s (Pörschke & Eigen, 1971; Craig et al., 1971; Pörschke et al., 1973). These increases in relaxation time reflect a variety of interactions and conformational restrictions. Of particular interest are the forces involved in helix formation. Base stacking is thought to contribute a dominant favorable energy term. The separation of the charged phosphates in the backbone decreases upon stacking and thus contributes an unfavorable electrostatic energy. Sugar puckering and backbone conformations may lead to significant entropy effects. In an effort to understand the contributions to helix formation, we have undertaken a study of the dynamics of nucleic acid stacking. This paper reports kinetic and thermodynamic results for the single-strand helix–coil transition of polyriboadenylic acid [poly(A)], polydeoxyriboadenylic acid [poly(dA)], and the ribo heptamer [$(Ap)_6A$]. The use of the laser temperature-jump method permits the study of these reactions at low salt concentrations and eliminates problems associated with the high electric fields used previously (Pörschke, 1973, 1978).

Experimental Section

Thermodynamics. The thermodynamics of the helix–coil transition were determined from an analysis of the temperature dependence of the ultraviolet absorbance. Melting curves were obtained from a Gilford 250 spectrophotometer interfaced to a PDP 11/34 computer. The temperature was varied from 2 to 85 °C with a heating rate of 30 °C/h. Over 300 data points were collected for each sample. All data were stored and analyzed by the computer. Absorbances were monitored at 260, 270, or 285 nm. All results are an average of at least three runs. Poly(A) and poly(dA) were incubated at 60 °C for 20 min before each run.

Kinetics. The observed chemical relaxations were less than 1 ms and required the use of the laser temperature-jump apparatus described previously (Dewey & Turner, 1978; Turner et al., 1972). The monochromator between the lamp and the sample had a spectral bandwidth of 10 nm. Schott UG3 and UG11 filters were placed in front of the phototube when the signal at 285 nm was observed. For 270-nm signals an Acton Research Corp. 260-nm (36-nm band-pass) interference filter was used. A 2-ms high-current pulse was applied to the xenon lamp to increase the light intensity (Turner et al., 1974). A photographic shutter limited the total sample exposure time to 20 ms/temperature jump. Relaxation times represent an average of at least 14 shots. A sample of poly(A) in D_2O was monitored to check against photochemical effects. The temperature jump in D_2O is 100 times less than in H_2O, and no signal was observed.

Chemicals. Poly(A) and poly(dA) were obtained from Sigma and dialyzed at least 48 h. The first 24 h was against a buffer containing 0.02 M EDTA, 0.05 M sodium cacodylate, and the desired sodium chloride concentration. The second 24 h was against buffer without EDTA. Buffers were changed twice in 24 h. $(Ap)_6A$ was purchased from Boehringer Mannheim. Purity was verified by paper chromatography. Poly(A) chromatography markers of specific length were purchased from Miles. As a check for degradation of the polymers, gel electrophoresis was run on the sample before and after a temperature-jump experiment. In 10% polyacrylamide gel (DeWachter & Fiers, 1971) the samples ran slightly slower than a 410-base average-length poly(A) marker and much slower than a 44-base average-length marker. The polymer

† From the Department of Chemistry, University of Rochester, Rochester, New York 14627. *Received July 6, 1979.* This work was supported by National Institutes of Health Grant GM 22939. D.H.T. is an Alfred P. Sloan Fellow.

[1] Abbreviations used: poly(A), polyadenylic acid; poly(dA), polydeoxyadenylic acid; $(A_p)_6A$, riboadenylic acid heptamer; EDTA, ethylenediaminetetraacetic acid.

0006-2960/79/0418-5757$01.00/0

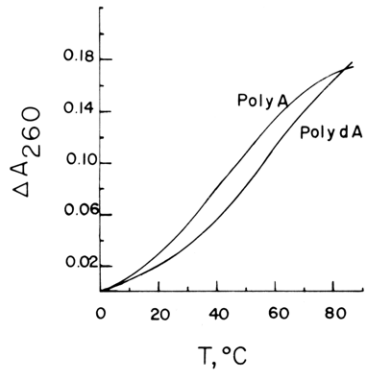

FIGURE 1: Change in absorbance at 260 nm with temperature for poly(A) and poly(dA) in 0.05 M sodium cacodylate. Initial absorbance is 0.35 for poly(A) and 0.61 for poly(dA) in a 1-cm path length cell.

length was maintained throughout the temperature-jump experiments. Similar checks were made before and after a melting curve experiment.

Results

Equilibrium. The change in absorbance with temperature for poly(A) and poly(dA) is shown in Figure 1. The melting curves were analyzed with a two-state model. The extinction coefficient of the sample is given by

$$\epsilon = \alpha(\epsilon_s - \epsilon_u) + \epsilon_u \quad (1)$$

where ϵ_s is the extinction of the totally stacked or helical state, ϵ_u is the unstacked or random-coil extinction, and α is the fraction of molecules in the helical state. The equilibrium constant for the coil to helix process is

$$K = \alpha/(1 - \alpha) = \exp[(-\Delta H/RT) + (\Delta S/R)] \quad (2)$$

When the melting transition is sharp enough, ϵ_u and ϵ_s are determined from the limiting extinctions at high and low temperatures, respectively. The data in Figure 1 show that for single-strand stacking, neither ϵ_s nor ϵ_u is well-defined. For avoidance of the problem of choosing a somewhat arbitrary base line, the entire melting curve was analyzed by a nonlinear least-squares fit to eq 1. This iterative procedure fits ϵ_u, ϵ_s, ΔH, and ΔS and calculates standard deviations for each parameter (Whittaker & Robinson, 1969). This algorithm was tested with computer-generated ideal data and was found to be extremely accurate. When a 0.5% random error was included in the generated data, the fitted values agreed with the original values to within the calculated standard deviation. Generally, the standard deviations in ΔH and ΔS were ±10%, while the standard deviations in extinctions were about ±1%.

There is a substantial difference between enthalpies measured for poly(A) stacking by spectroscopic and calorimetric methods. It is therefore important to consider potential problems with the above analysis. Difficulties may arise if the extinction coefficients have a temperature dependence. The temperature dependence of the absorbance of adenine and adenosine was monitored at 260 nm. Both showed a linear decrease in absorbance of 5% over the range from 5 to 70 °C. This may be taken as a rough estimate of the temperature dependence of ϵ_u. Temperature-dependent extinctions were also included in the computer-generated data for the case when ϵ_u is 30% larger than ϵ_s. These conditions are very similar to the actual experimental results. Any combination of linear changes of ±5% in the extinctions resulted in larger standard deviations for each parameter. The fitted parameters were still within a standard deviation of the values used to generate the data. If either or both extinctions changed by ±10%, the algorithm failed to converge. The performance of the program with the computer-generated data shows that it would reliably fit the experimental data if the temperature dependence of the extinctions were small. The fitted values for the experimental data and their standard deviations are shown in Table I. The standard deviation of about ±12% for the enthalpy and entropy suggests that the temperature effects on extinction coefficients are small. If this was not true, then an instantaneous absorbance change should be observed in the relaxation experiments. The relaxations at 270 nm may show an instantaneous jump, whereas those at 285 nm do not (see Figure 2). The magnitude of the effect at 270 nm is less than 20% of the signal amplitude. This again indicates that the temperature de-

Table I: Thermodynamics of the Coil–Helix Transition

polymer	salt	λ (nm)	$-\Delta H$ (kcal/mol)	$-\Delta S$ (eu)
poly(A)	0.05 M sodium cacodylate	260	11.3 ± 1.1	36.3 ± 3
		270	11.8 ± 1.5	38.0 ± 5
		285	10.9 ± 1.6	35.7 ± 5
$(Ap)_6A$	0.05 M sodium cacodylate	260	9.8 ± 1.6	31.8 ± 5
poly(dA)	0.05 M sodium cacodylate	260	9.0 ± 1.0	26.5 ± 3
poly(A)	0.1 M NaCl, 0.1 M sodium cacodylate	260	9.6 ± 0.9	30.3 ± 3
		285	8.6 ± 2.4	27.8 ± 8

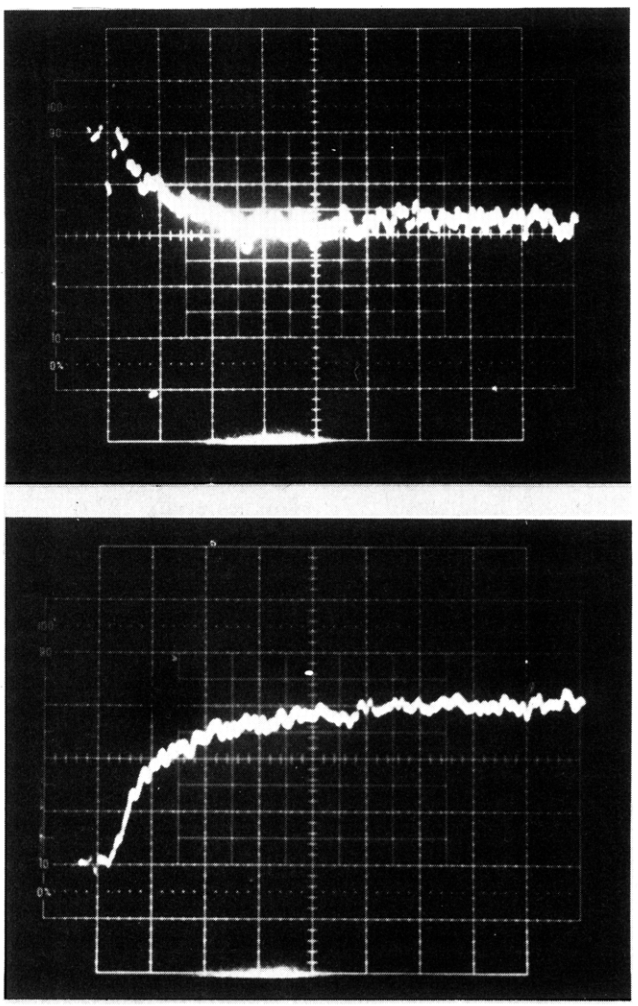

FIGURE 2: Relaxations observed for poly(A) at 25 °C in 0.05 M sodium cacodylate. Horizontal scale is 100 ns/division. (Top) Relaxation at 285 nm; (bottom) relaxation at 270 nm.

Table II: Relaxation Times of Poly(A) and $(Ap)_6A$ at 25 °C

polymer	salt	τ_{270} (ns)	τ_{285} (ns)
poly(A)	0.5 M sodium cacodylate	95 ± 16	105 ± 13
$(Ap)_6A$	0.5 M sodium cacodylate	113 ± 31	109 ± 33
poly(A)	0.1 M NaCl, 0.1 M sodium cacodylate	150 ± 30	270 ± 70
$(Ap)_6A$	0.1 M NaCl, 0.1 M sodium cacodylate	80 ± 30	280 ± 30
poly(A)	0.1 M NaCl, 0.1 M sodium cacodylate, 2 mM $MgCl_2$	200 ± 40	
poly(A)	0.1 M NaCl, 0.1 M sodium cacodylate, 5 mM $MgCl_2$	270 ± 80	

pendence of the extinction coefficients will not greatly affect the melting curves. Thus, a more fundamental reason must be found to explain the discrepancy between thermodynamics derived from spectroscopic and calorimetric results.

At 0.05 M ionic strength, the poly(A) results are independent of the wavelength monitored. The enthalpy of −11.3 kcal/mol compares favorably with values obtained by spectroscopic methods for a variety of conditions (−9 to −13 kcal/mol) (Leng & Felsenfeld, 1966; Poland et al., 1966; Applequist & Damle, 1966; Pörschke, 1971; Stannard & Felsenfeld, 1975). However, these values differ greatly from the enthalpy of −2.7 to −4.2 kcal/mol determined by calorimetry (Rawitscher et al., 1963; Neumann & Ackermann, 1968). Calorimetric data analyzed with a nearest-neighbor Ising model give a ΔH of −8.5 kcal/mol, a T_m of 45 °C, and a cooperativity parameter, σ, of 0.57 (Suurkuusk et al., 1977). The van't Hoff enthalpy is related to the cooperative model enthalpy by

$$\Delta H_{vH} = \Delta H_{coop}/\sigma^{1/2} \quad (3)$$

Thus, a cooperative model enthalpy of −8.5 kcal/mol corresponds to a van't Hoff enthalpy of −11.3 kcal/mol, in excellent agreement with our results.

The heptamer shows similar thermodynamics to the polymer, as is expected for a transition of such low cooperativity. Similar results were obtained previously on the thermodynamics as a function of chain length for poly(A) (Poland et al., 1966). Again, the spectroscopic results differ considerably from the enthalpy of −2.9 kcal/mol determined calorimetrically between 0 and 70 °C (Breslauer & Sturtevant, 1977).

The high melting temperature of poly(dA) is consistent with qualitative observations in the literature (Ts'o et al., 1966; Riley et al., 1966; Barszcz & Shugar, 1968; Alderfer & Smith, 1971). However, there are few quantitative results. One spectroscopic study gives a van't Hoff enthalpy of less than 5.0 kcal/mol, as compared with our value of 9.0 kcal/mol (Vournakis et al., 1967).

Kinetics. The results of the kinetic measurements are shown in Tables II and III. Figure 2 shows typical relaxation traces at the two wavelengths monitored. For poly(A) in 0.05 M sodium cacodylate at 270 nm and 15 °C, relaxations for base concentrations of 36.4, 9.11, and 1.82 mM were observed to be 123 ± 24, 125 ± 36, and 132 ± 23 ns, respectively. This indicates that the observed process is unimolecular. Three different poly(A) sample lots were measured at 270 nm under the same conditions. The three observed relaxation times were 129 ± 27, 125 ± 36, and 133 ± 13 ns. Our results for this buffer were independent of wavelength. Table III shows the temperature dependence of this relaxation for poly(A) and $(Ap)_6A$. The results are very similar for the polymer and oligomer, as expected for a transition of low cooperativity.

For ionic strengths near 0.2 M, the relaxation time was observed to be wavelength dependent for poly(A) and $(Ap)_6A$.

Table III: Temperature Dependence of Relaxation Times[a] in 0.05 M Sodium Cacodylate

	$(Ap)_6A$		poly(A)		poly(dA),
T (°C)	270 nm	285 nm	270 nm	285 nm	270 nm
5	209 ± 35				52 ± 15
10	156 ± 21		174 ± 19		48 ± 13
15	126 ± 37		126 ± 15	126 ± 19	44 ± 11
25	113 ± 31	109 ± 33	95 ± 16	105 ± 13	32 ± 7
35			64 ± 12	57 ± 10	

[a] In nanoseconds.

These results are shown in Table II. Because of this wavelength dependence, it is not possible to obtain individual rate constants from the data. In general, relaxation times get longer with increasing ionic strength. Addition of millimolar amounts of Mg^{2+} also increased the relaxation time (see Table II).

For poly(dA) the absorbance change at wavelengths longer than 280 nm was too small to resolve a relaxation signal. The relaxation times at 270 nm are given in Table III for 0.05 M sodium cacodylate.

Our results at 0.2 M ionic strength are in general agreement with those measured previously using a cable-discharge temperature-jump apparatus (Pörschke, 1973, 1978). Additional measurements on oligoriboadenylic acids at 1 M ionic strength are also in qualitative agreement with recent results (Pörschke, 1978). However, our results at 0.05 M ionic strength are considerably different from these previous studies. Artifacts were detected in the cable-discharge temperature-jump study due to orientation of the polymers in the high electric fields. Such effects increase at low ionic strength. The laser temperature-jump technique avoids this problem, which probably accounts for the discrepancy.

The low salt results were analyzed with a two-state model. The relaxation time, τ, for a two-state, unimolecular reaction is given by

$$1/\tau = k_1 + k_{-1} \quad (4)$$

where k_1 is the rate of helix formation and k_{-1} is the rate of coil formation. The equilibrium constants determined spectroscopically were used to partition the relaxation time into a forward and reverse rate. Activation entropies, $\Delta S^{\ddagger}$, were determined at 25 °C by using the Eyring equation

$$k = (eRT/hN) \exp(\Delta S^{\ddagger}/R) \exp(-E_a^{\ddagger}/RT) \quad (5)$$

The kinetic data were also analyzed by using the cooperative model of Schwarz (1965). This model requires independent knowledge of the cooperativity parameter, σ. For poly(A), σ was suggested to be 0.5 on theoretical grounds (Applequist & Damle, 1966) and was determined to be 0.57 experimentally (Suurkuusk et al., 1977). In general, a cooperative kinetic model will result in four relaxation processes, not all of which have significant amplitudes (Schwarz, 1972). However, a mean relaxation time can be calculated from

$$1/\tau^* = k_f[(s-1)^2 + 4\sigma s]/[s/2[(1+s) + [(1-s)^2 + 4\sigma s]^{1/2}]] \quad (6)$$

where k_f is the rate for adding a stacked unit onto a helical sequence and s is the equilibrium constant for this growth process. The reverse rate, k_r, is s/k_f, and the rate of helix initiation is σk_f. Although τ^* is a mean relaxation time, it gives the exact result for a two-state model in the limit of $\sigma = 1$. The error in the difference between τ^* and the true τ can easily be estimated (Schwarz, 1965). Assuming $\sigma = 0.5$, this error is less than 10%, well within experimental error for

Table IV: Rate Constants and Activation Parameters in 0.05 M Sodium Cacodylate for the Two-State and Kinetic Ising Models[a]

T (°C)	$k_{-1} \times 10^{-6}$ (s^{-1})	$k_1 \times 10^{-6}$ (s^{-1})
	Poly(A)	
10	0.8 (1.6)	4.9 (6.2)
15	1.5 (2.7)	6.4 (8.5)
25	3.2 (5.5)	7.0 (10.6)
35	7.4 (12.3)	9.2 (15.8)
E_a (kcal/mol)	15.2 (14.1)	4.0 (6.2)
$\Delta S^{\ddagger}$ (eu)	20.3 (17.6)	−15.8 (−7.5)
	Poly(dA)	
5	0.9 (2.8)	18 (23)
10	1.4 (3.4)	19 (22)
15	1.9 (4.5)	21 (24)
25	4.3 (9.2)	27 (34)
E_a (kcal/mol)	12.3 (9.6)	3.2 (3.3)
$\Delta S^{\ddagger}$ (eu)	11.1 (3.3)	−15.8 (−15.1)
	$(Ap)_6A$	
5	0.7 (1.5)	4.0 (5.1)
10	1.3 (2.5)	5.4 (6.9)
15	2.0 (3.9)	6.1 (8.4)
25	3.3 (6.1)	5.6 (8.8)
E_a (kcal/mol)	12.3 (10.8)	2.5 (3.7)
$\Delta S^{\ddagger}$ (eu)	10.6 (8.9)	−21.1 (−14.1)

[a] Values for the kinetic Ising model are given in parentheses, and values outside the parentheses are for the two-state model.

the conditions of the poly(A) experiments. The thermodynamics for the growth process were obtained from eq 3, assuming $\sigma = 0.5$, and from the experimentally determined T_m. The k_f and k_r values are listed in Table IV along with the activation parameters. The least-squares fits to the Eyring equation for k_f and k_r are shown in the supplementary material (see paragraph at end of paper in regard to supplementary material).

With both of the above analyses, the activation energies for helix formation are 3–6 kcal/mol and a significant unfavorable activation entropy is found. The reverse rates show a considerable potential well of between 10 and 15 kcal/mol for the stacked conformation and exhibit a favorable entropy of activation. These parameters can provide insight into the interactions controlling these processes.

Discussion

The low salt regime affords a detailed analysis since a single relaxation is observed. The forward rate for both poly(A) and poly(dA) shows a low activation energy (3–6 kcal/mol) and yet is only 10^6–10^7 s^{-1}. This suggests an unfavorable entropy of activation. Although backbone rotations are on a 10^{-8}–10^{-10}-s time scale, helix formation is much slower. This difference can be largely accounted for by the entropy of restriction of internal rotational degrees of freedom necessary to form the transition state. The transition state may be viewed as one rotamer crossing a single rotational barrier while all other rotamers in the backbone are in a fixed configuration. There are six backbone rotations plus the sugar–base rotation to be considered (Sundaralingam, 1973, 1975). Thus, for example, the preexponential term may correspond to a torsional vibrational frequency of the base–sugar bond rotation. Torsional vibrational frequencies are usually on the order of 10^{12} s^{-1} (Wyn-Jones & Orville-Thomas, 1972). A large unfavorable entropy term could arise because all the backbone rotational degrees of freedom are restricted in the transition state. In the simplest approximation, rotations have three states (two gauche and one trans) (Flory, 1953), and the restriction to one degree gives an activation entropy of

$$\Delta S^{\ddagger} = -nR \ln 3 \quad (7)$$

where n is the number of rotations that are restricted. This term arises in transition-state theory from the degeneracies of the torsional vibrational partition functions. For poly(A), the measured $\Delta S^{\ddagger}$ is −15.8 or −7.5 eu for the two-state or Ising model, respectively. This corresponds to seven or three restricted rotations. The Ising model gives a growth rate and therefore should require the restriction of one less degree of freedom. For poly(dA), both models yield seven restricted rotations. However, this may be due to $\sigma = 0.5$ being inappropriate for poly(dA). It has been suggested that σ is greater than 1.0 for poly(dA) (Vournakis et al., 1967).

X-ray structure, NMR, and potential energy calculation studies all indicate that several of the backbone rotations have fewer than three states at equilibrium (Sundaralingam, 1973, 1975; Kim et al., 1973; Kondo & Danyluk, 1976; Lee et al., 1976; Olson, 1979). By use of the notation of Sundaralingam for the various dihedral angles, a more realistic counting of states is $\chi(3)$, $\phi,\phi'(1)$, $\psi(3)$, $\psi'(2)$, and $\omega\omega'(6)$ (Sundaralingam, 1973, 1975). Restriction of the transition state to one conformation then gives a $\Delta S^{\ddagger} = -R \ln (3 \times 3 \times 2 \times 6) = -9.3$ eu. Another way of theoretically estimating $\Delta S^{\ddagger}$ is from entropies of bond fusion in linear polymers. The entropies range from 1.3 to 3.0 eu, which would suggest between 5 and 13 restricted rotations (Flory, 1953). Thus, conformational effects can account for most of the activation entropy, whatever the model. This suggests that solvent and salt effects are relatively unimportant in determining the forward rate. The similarity of the forward rate and activation entropy of polycytidylic acid stacking at 1.05 M ionic strength (1.1×10^7 s^{-1} and −19.4 eu, respectively) with those measured for poly(A) at 0.05 M ionic strength also supports this conclusion (Pörschke, 1976).

The forward rate constants for poly(dA) are about a factor of 4 faster than those for the ribopolymer. The activation energy is 0.8 kcal/mol lower for poly(dA). While this is within the error of our measurement, it may reflect the difference in the barriers for base–sugar rotation. Relaxation times for syn–anti isomerization are twice as long for adenosine as for 2′-deoxyadenosine. This is consistent with our results. Since the forward rate seems to be controlled by backbone interactions, the rates determined may prove to be limiting rates for conformational changes in nucleic acids. The differences in forward rates suggest that the backbone is more flexible for deoxypolymers than for ribopolymers. This flexibility may explain the greater stability of short deoxy hairpin helices relative to ribo hairpins (Scheffler et al., 1970; Gralla & Crothers, 1973).

The reverse rates are characterized by a large activation energy. This probably reflects a substantial contribution from base stacking. If the forward rate activation energy is a measure of the rotational barriers, then this can be subtracted from the reverse rate activation energy to give a stacking energy of ~10 kcal/mol. This is also, of course, the equilibrium enthalpy for the reactions. Thus, the low value of E_a for the forward rate is consistent with the popular idea that stacking interactions dominate the overall thermodynamics. There is also a large favorable activation entropy for the reverse rate. This may be due to electrostatic and solvation effects.

The salt effects on the kinetics of poly(A) are not easily interpreted. The wavelength-dependent relaxation times at higher salt suggest that at least three states are involved in the reaction. The shift from two to more states is not unexpected based on Manning's polyelectrolyte theory (Manning,

1978). This theory predicts that the local salt concentration around helical poly(A) will be 0.35 M as long as the bulk solvent salt concentration is much less than this. The shift in relaxation behavior observed between 0.05 and 0.2 M suggests that the local salt concentration is changing. This is not surprising since poly(A) near 25 °C is a mixture of stacked and unstacked residues whereas the calculation assumes a completely stacked polymer with a 3.1-Å phosphate spacing. Also, 0.2 M does not meet the theoretical criterion of being much less than 0.35 M. For any three-state model the sum of the reciprocal relaxation times equals the sum of the rate constants for all the processes. Making the major assumption that the relaxation times measured at the two wavelengths are independent, the sum of reciprocal relaxation times at 25 °C is 1.04×10^7 s^{-1}. This represents the sum of the individual rate constants. At low salt the forward and reverse rate constants were determined to be 7.0×10^6 and 3.2×10^6 s^{-1}, respectively. The activation energy for k_1 suggests that it has a very small barrier and is not limited by unfavorable electrostatic effects. Since the forward rate is dominated by conformational entropy effects, it is reasonable to assume that k_1 will be independent of ionic strength. To allow for realistic rate constants associated with the third state, the reverse rate must decrease with salt. It appears that a stacked conformation is stabilized by higher salt. The stacked state requires a shortening of the phosphate–phosphate distance to the nearest neighbors, and screening effects may be important. Unfortunately, from these data alone it is difficult to characterize the third state.

The relaxation times for poly(A) become slower on addition of small amounts of Mg^{2+}. As with the monovalent salt effects, this may be viewed as stabilizing the stacked form and slowing the reverse rate. The higher charge on Mg^{2+} is much more effective in screening the phosphate backbone.

From this study it is seen that salt effects on the kinetics of the single-stranded helix–coil transformation are considerably more complex than the equilibrium data would suggest. It appears that stacked conformations are stabilized to some extent by electrostatic screening. These effects are difficult to quantitate because of additional stable conformations introduced at high salt. The elucidation of the various interactions contributing to the stability of the stacked conformations awaits additional experiments with different solvents and base composition. This work has characterized the forward rate as being dominated by a conformational entropy barrier. In the future the kinetic approach should be invaluable in determining the factors affecting the reverse rate.

Acknowledgments

We thank Craig Hall for his expert help in starting this work and Drs. W. K. Olson, G. S. Manning, and K. J. Breslauer for helpful comments.

Supplementary Material Available

One figure showing the melting curve for $(Ap)_6A$ and three figures showing Eyring plots of poly(A), poly(dA), and $(A_p)_6A$ for both the two-state and kinetic Ising models (4 pages). Ordering information is given on any current masthead page.

References

Akasaka, K. (1974) *Biopolymers 13*, 2273.

Alderfer, J. L., & Smith, S. L. (1971) *J. Am. Chem. Soc. 93*, 7305.

Applequist, J., & Damle, V. (1966) *J. Am. Chem. Soc. 88*, 3895.

Barszcz, J. L., & Shugar, S. (1968) *Eur. J. Biochem. 5*, 91.

Breslauer, K. J., & Sturtevant, J. M. (1977) *Biophys. Chem. 7*, 205.

Craig, M. E., Crothers, D. M., & Doty, P. (1971) *J. Mol. Biol. 62*, 383.

Davanloo, P., Armitage, I. M., & Crothers, D. M. (1979) *Biopolymers 18*, 663.

DeWachter, R., & Fiers, W. (1971) *Methods Enzymol. 21*, 167.

Dewey, T. G., & Turner, D. H. (1978) *Adv. Mol. Relaxation Processes 13*, 331.

Flory, P. F. (1953) in *Principles of Polymer Chemistry*, Cornell University Press, Ithaca, NY.

Gralla, J., & Crothers, D. M. (1973) *J. Mol. Biol. 73*, 497.

Hemmes, P. R., Oppenheimer, L., & Jordan, F. (1974) *J. Am. Chem. Soc. 96*, 6023.

Kim, S. H., Berman, H. M., Seeman, S. C., & Newton, M. D. (1973) *Acta Crystallogr., Sect. B 29*, 703.

Kondo, N. S., & Danyluk, S. S. (1976) *Biochemistry 15*, 756.

Lee, C. H., Ezra, F. S., Kondo, N. S., Sarma, R. H., & Danyluk, S. S. (1976) *Biochemistry 15*, 3627.

Leng, M., & Felsenfeld, G. (1966) *J. Mol. Biol. 15*, 455.

Manning, G. S. (1978) *Q. Rev. Biophys. 11*, 2, 179.

Neumann, E., & Ackermann, T. (1969) *J. Phys. Chem. 73*, 2170.

Olson, W. K. (1979) *Proceedings of the International Symposium on Biomolecular Structure, Conformation, Function and Evolution* (Srinivasan, R., Ed.) Pergamon Press, Elmsford, NY (in press).

Poland, D., Vournakis, J. N., & Scheraga, H. A. (1966) *Biopolymers 4*, 223.

Pörschke, D. (1971) *Biopolymers 10*, 1989.

Pörschke, D. (1973) *Eur. J. Biochem. 39*, 117.

Pörschke, D. (1976) *Biochemistry 15*, 1495.

Pörschke, D. (1978) *Biopolymers 17*, 315.

Pörschke, D., & Eigen, M. (1971) *J. Mol. Biol. 62*, 361.

Pörschke, D., Uhlenbeck, O. C., & Martin, F. H. (1973) *Biopolymers 12*, 1313.

Rawitscher, M. A., Ross, P. D., & Sturtevant, J. M. (1963) *J. Am. Chem. Soc. 85*, 1915.

Rhodes, L. M., & Schimmel, P. R. (1971) *Biochemistry 10*, 4426.

Riley, M., Maling, B., & Chamberlain, M. J. (1966) *J. Mol. Biol. 20*, 359.

Scheffler, I. E., Elson, E. L., & Baldwin, R. L. (1970) *J. Mol. Biol. 48*, 145.

Schwarz, G. (1965) *J. Mol. Biol. 11*, 64.

Schwarz, G. (1972) *J. Theor. Biol. 36*, 569.

Stannard, B. S., & Felsenfeld, G. (1975) *Biopolymers 14*, 299.

Sundaralingam, M. (1973) *Jerusalem Symp. Quantum Chem. Biochem. 5*, 417.

Sundaralingam, M. (1975) in *Structure and Conformation of Nucleic Acids and Protein–Nucleic Acid Interactions* (Sundaralingam, M., & Rao, S. T., Eds.) p 487, University Park Press, Baltimore, MD.

Suurkuusk, J., Alvarez, J., Freire, E., & Biltonen, R. L. (1977) *Biopolymers 16*, 2641.

Ts'o, P. O., Rapaport, S. A., & Bollum, F. J. (1966) *Biochemistry 5*, 4153.

Turner, D. H., Flynn, G. W., Sutin, N., & Beitz, J. V. (1972) *J. Am. Chem. Soc. 94*, 1554.

Turner, D. H., Yuan, R., Flynn, G. W., & Sutin, N. (1974) *Biophys. Chem. 2*, 385.
Vournakis, J. N., Poland, D., & Scheraga, H. A. (1967) *Biopolymers 5*, 403.
Whittaker, E., & Robinson, G. (1969) in *The Calculus of Observations*, 4th ed., p 164, Blackie, Glasgow, U.K.
Wyn-Jones, E., & Orville-Thomas, W. J. (1972) *Adv. Mol. Relaxation Processes 2*, 201.

Binding of Platinum(II) Intercalation Reagents to Deoxyribonucleic Acid. Dependence on Base-Pair Composition, Nature of the Intercalator, and Ionic Strength†

Mary Howe-Grant‡ and Stephen J. Lippard*

ABSTRACT: The DNA binding of three platinum(II) intercalation reagents has been studied and found to depend upon base composition, the nature of the intercalator, and the ionic strength of the solvent medium. In 0.2 M NaCl, binding data for calf thymus DNA show the association constants to be $\sim 10^4$ M^{-1}. The binding constants decrease in the order [(*o*-phen)Pt(en)]$^{2+}$ ≥ [(terpy)Pt(HET)]$^+$ ≫ [(bipy)Pt(en)]$^{2+}$. The number of available intercalation sites for the doubly charged intercalators is only 70% of the number expected from the nearest-neighbor exclusion model. Binding of [(*o*-phen)Pt(en)]$^{2+}$ and [(terpy)Pt(HET)]$^+$ to various DNAs depends linearly on G·C content. Both reagents exhibit essentially the same degree of G·C specificity. Intercalative binding is a function of ionic strength. Increasing the salt concentration minimizes the importance of metallointercalator charge, and extrapolation to 1 M salt reveals the intercalative abilities, as reflected in binding constants, to be equivalent for [(terpy)Pt(HET)]$^+$ and [(*o*-phen)Pt(en)]$^{2+}$ and about 1 order of magnitude less than that of ethidium.

Platinum(II) complexes containing aromatic ligands coplanar with the metal coordination sphere bind intercalatively to double-stranded DNAs, while noncoplanar-aromatic and planar-nonaromatic complexes do not (Jennette et al., 1974; Howe-Grant et al., 1976; Lippard et al., 1976; Nordén, 1978; Lippard, 1978). Intercalation is a mode of nucleic acid binding for a variety of drugs and antibiotics, many of which are frameshift mutagens or inhibitors of DNA synthesis (Waring, 1968). This binding mode has been postulated for protein–nucleic acid recognition in vivo (Gabbay et al., 1973; Coleman & Armitage, 1978; Maurizot et al., 1978). Because of their high electron density, platinum intercalation reagents have been used to investigate nucleic acid structure and the intercalative binding mode itself. X-ray fiber diffraction studies of DNA containing bound metallointercalators (Bond et al., 1975; Lippard et al., 1976) and a crystal structure determination of the platinum intercalation reagent [(terpy)Pt(HET)]$^+$ [1] (Figure 1) contained within a segment of double-helical DNA (Wang et al., 1978) have helped to clarify the frequency and distribution of bound intercalators at saturation, the total number of sites available to an intercalation reagent along the DNA helix, and the sugar puckering and unwinding angle of DNA in the intercalation complex. The [(terpy)Pt(HET)]$^+$ cation also inhibits genetic recombination in pneumococci (Seto & Tomaz, 1977).

The present study examines several factors involved in the binding of platinum intercalators to DNA. The relative importance of intercalator structure, DNA base composition, and electrostatic charge interactions is elucidated by varying the nature of the metal complex (see Figure 1), the DNA, and the ionic strength of the solvent medium.

Materials and Methods

Metal Complexes. The compounds [(terpy)Pt(HET)]NO_3 (Howe-Grant & Lippard, 1980), [(*o*-phen)Pt(en)]$(NO_3)_2$ (Howe-Grant, 1978), [(bipy)Pt(en)]$(NO_3)_2$ (Erickson, 1969), and [$(py)_2$Pt(en)]$(ClO_4)_2$ (Appleton & Hall, 1971) were prepared by published procedures. Tritiated complexes were synthesized from [^{3}H]-2,2′,2″-terpyridine or [^{3}H]-1,10-phenanthroline supplied by New England Nuclear Co. The radiolabeled ligands were diluted with unlabeled material in ethanol or equimolar ethanol–benzene solutions and isolated after precipitation with water. Purity of the labeled complexes was determined spectrophotometrically.

Concentrations of stock solutions containing metal complexes were determined spectrophotometrically in water or the appropriate buffer on the basis of reported molar extinction coefficients (Howe-Grant, 1978).

Buffers and Other Chemicals. All experiments were carried out at pH 7.5 in buffer 1 (10 mM sodium chloride and 10 mM Tris-HCl), buffer 2 (100 mM sodium chloride and 50 mM Tris-HCl), buffer 3 (200 mM sodium chloride and 50 mM Tris-HCl), buffer 3′ (200 mM sodium chloride, 50 mM Tris-HCl, and 1 mM EDTA), buffer 4 (190 mM sodium chloride and 10 mM Tris-HCl), buffer 5 (5 mM sodium

† From the Department of Chemistry, Columbia University, New York, New York 10027. *Received June 5, 1979.* This work was supported by U.S. Public Health Service Grant CA-15826 from the National Cancer Institute.

‡ A National Institutes of Health National Research Service Award recipient, Training Grant No. GM-07216.

[1] Abbreviations used: EtdBr, ethidium bromide; bipy, 2,2′-bipyridine; en, ethylenediamine; *o*-phen, 1,10-phenanthroline; terpy, 2,2′,2″-terpyridine; py, pyridine; HET, 2-hydroxyethanethiolate; EDTA, disodium salt of ethylenediaminetetraacetic acid; Tris, tris(hydroxymethyl)-aminomethane; *r*, ratio of bound metal to nucleotide concentrations; P_0, concentration of nucleotide; C_B, C_F, C_T, concentrations of bound, free, and total intercalator, respectively; C_{obsd}, observed concentration of free intercalator, equal to C_F provided that no C_D, dimerized free intercalator, is present in solution.

0006-2960/79/0418-5762$01.00/0